ODA16 aids axonemal outer row dynein assembly through an interaction with the intraflagellar transport machinery

Noveera T. Ahmed,[1] Chunlei Gao,[1] Ben F. Lucker,[2] Douglas G. Cole,[2] and David R. Mitchell[1]

[1]Department of Cell and Developmental Biology, State University of New York Upstate Medical University, Syracuse, NY 13210
[2]Department of Microbiology, Molecular Biology and Biochemistry, University of Idaho, Moscow, ID 83844

Formation of flagellar outer dynein arms in *Chlamydomonas reinhardtii* requires the ODA16 protein at a previously uncharacterized assembly step. Here, we show that dynein extracted from wild-type axonemes can rebind to *oda16* axonemes in vitro, and dynein in *oda16* cytoplasmic extracts can bind to docking sites on *pf28* (oda) axonemes, which is consistent with a role for ODA16 in dynein transport, rather than subunit preassembly or binding site formation. ODA16 localization resembles that seen for intraflagellar transport (IFT) proteins, and flagellar abundance of ODA16 depends on IFT. Yeast two-hybrid analysis with mammalian homologues identified an IFT complex B subunit, IFT46, as a directly interacting partner of ODA16. Interaction between *Chlamydomonas* ODA16 and IFT46 was confirmed through in vitro pull-down assays and coimmunoprecipitation from flagellar extracts. ODA16 appears to function as a cargo-specific adaptor between IFT particles and outer row dynein needed for efficient dynein transport into the flagellar compartment.

Introduction

Cilia and flagella are complex microtubule-based organelles composed of several hundred proteins (Li et al., 2004; Pazour et al., 2005). Failure to properly assemble just a single flagellar complex, such as outer arm dynein, results in primary ciliary dyskinesia in humans, which has been linked to chronic sinopulmonary infections, reduced male fertility, and congenital organogenesis abnormalities due to defects in embryonic left–right asymmetry determination (Zariwala et al., 2007). Assembly of these organelles is a multistep process involving partial preassembly of complexes in the cytoplasm, transport of proteins and protein complexes into the flagellar compartment, assembly of a framework of outer doublet and central pair microtubules, and attachment of other components onto the microtubule framework. For example, outer dynein arms (Fowkes and Mitchell, 1998) and radial spokes (Qin et al., 2004) both undergo preassembly in the cytoplasm before entering the flagellar compartment. This process has been extensively studied in *Chlamydomonas reinhardtii* through the analysis of mutations that disrupt assembly of specific flagellar structures (Silflow and Lefebvre, 2001; Kamiya, 2002; Dutcher, 2003) and through studies of the intraflagellar transport (IFT) machinery essential to flagellar assembly and maintenance (Cole, 2003; Scholey, 2003).

Recent analysis of an *ift46* mutant supports an IFT requirement for outer arm dynein assembly. IFT46 is an IFT complex B protein whose absence in the *ift46-1* strain results in very short flagella that lack many normal structures, including inner and outer row dyneins (Hou et al., 2007). A partial suppressor strain that expresses a truncated form of IFT46, $sup_{ift46}1$, assembles flagella of variable lengths that retain wild-type levels of inner arm dynein but fail to assemble outer arm dynein (Hou et al., 2007), which suggests that IFT46 plays an essential role in outer arm dynein assembly, and that ODAs require a unique interaction with IFT particles for their proper transport into flagella. Here, we provide evidence that the protein product of the *ODA16* dynein assembly locus may regulate the link between outer arm dynein and IFT46, and thus ODA16 represents the first identified adaptor between an IFT cargo and an IFT subunit.

Most of the 17 characterized *C. reinhardtii* outer arm dynein assembly loci encode proteins specifically needed as subunits of one of two axonemal complexes, the dynein motor itself,

Correspondence to David R. Mitchell: mitcheld@upstate.edu

Abbreviations used in this paper: IFT, intraflagellar transport; ODA-HC and ODA-IC, outer arm dynein heavy chain and intermediate chain, respectively.

© 2008 Ahmed et al. This article is distributed under the terms of an Attribution–Noncommercial–Share Alike–No Mirror Sites license for the first six months after the publication date (see http://www.jcb.org/misc/terms.shtml). After six months it is available under a Creative Commons License (Attribution–Noncommercial–Share Alike 3.0 Unported license, as described at http://creativecommons.org/licenses/by-nc-sa/3.0/).

The Rockefeller University Press $30.00
J. Cell Biol. Vol. 183 No. 2 313–322
www.jcb.org/cgi/doi/10.1083/jcb.200802025

or a docking complex that forms a dynein attachment site on the doublet surface (Fowkes and Mitchell, 1998; Kamiya, 2002). The *ODA5* locus may encode a subunit of a third axonemal complex needed for dynein binding (Wirschell et al., 2004). However, some *ODA* loci do not apparently encode axonemal proteins and may therefore be directly involved in the assembly process. Here, we test the function of one such locus, *ODA16*, that does not appear to encode an axonemal protein, and which has other unique properties more consistent with a role in assembly or transport of the dynein motor (Ahmed and Mitchell, 2005). *Chlamydomonas* strains harboring mutations at *ODA16* fail to assemble a full compliment of outer arm dyneins onto axonemes, but show normal complementation in temporary diploids between *oda16* gametes and gametes with defects in cytoplasmic preassembly of the motor, docking, or accessory complexes needed for outer dynein arm assembly. This indicates that these complexes are likely unaffected by the *oda16* mutation. In addition, the few outer arm dyneins that do assemble on *oda16* axonemes appear functional (i.e., contribute to motility). Here, we eliminate several possible roles for the ODA16 protein during outer arm dynein assembly by showing that it does not act as a chaperone for doublet attachment, as a factor that modifies dynein to an assembly competent form, or as an axonemal docking site needed for outer arm dynein attachment. Instead, our results suggest that ODA16 assists in dynein transport from the cytoplasm into the flagellar compartment through an interaction with IFT46. Our data are consistent with a hypothesis that some axonemal components, including outer arm dynein, are released immediately upon transport into the flagellar compartment.

Results

Oda16 outer arm dyneins

Chlamydomonas oda16 strains only assemble 10–20% of the wild-type amount of outer arm dynein into flagella, but this small remaining amount of dynein forms a strong attachment to axonemal microtubules and contributes to flagellar motility (Ahmed and Mitchell, 2005). Our previous electron microscopic analysis of *oda16* axonemes revealed variable numbers of outer row dynein arms per cross section but did not determine whether this represented a truly random variation or a proximal-distal gradient in dynein assembly. To see if the remaining outer arm dyneins in *oda16* flagella assemble preferentially near the base or tip of the axoneme, wild-type and *oda16* cells were compared using immunofluorescence with an antibody against an outer arm dynein intermediate chain (ODA-IC), ODA-IC2 (Fig. 1, A and B). As expected, dynein in wild-type cells is evenly distributed along both flagella and is also seen as a dispersed signal in the cell body. Fluorescence signal intensity was greatly decreased in *oda16* flagella, but its distribution was identical to that observed in wild-type flagella, which is consistent with an apparently random distribution of the remaining outer arms. The distribution of the dynein signal in *oda16* cell bodies remained nonlocalized as in wild-type cells, but its intensity was increased in *oda16* cells compared with wild-type cells.

We hypothesized that reduced flagellar outer arm assembly might result if *oda16* axonemes have reduced numbers of functional binding sites for dynein attachment or if the dynein complexes transported into *oda16* flagella are unable to bind efficiently. To test whether the remaining unoccupied outer dynein arm attachment sites in *oda16* flagella were capable of binding wild-type outer arm dynein in vitro, a high-salt extract of isolated, demembranated wild-type axonemes, which contains outer arm dynein but lacks ODA16 (Ahmed and Mitchell, 2005), was dialyzed to remove salt and incubated with *oda16* axonemes. After separation of axonemes from unbound dynein by centrifugation, the amount and specificity of dynein binding was assessed by Western blotting and electron microscopy of the pelleted axoneme fraction. As shown in Fig. 2 (A–C), outer arm dynein was restored to wild-type levels and appearance on these *oda16* axonemes. Therefore, ODA16 is not needed to modify axonemes for outer arm dynein attachment.

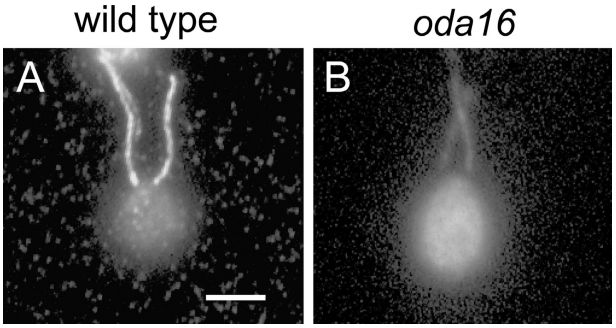

Figure 1. **Outer arm dynein distribution in the absence of ODA16.** Immunofluorescence images of wild-type (A) and *oda16* (B) cells stained with anti–ODA-IC2 show uniform distribution of outer arm dynein along the length of the flagella in both strains, although signal intensity is lower in the mutant flagella. Cytoplasmic distribution of ODA-IC2 is also similar in both strains, but abundance appears greater in mutant cytoplasm. Bar, 5 µm.

To test the alternative that ODA16 alters outer arm dynein into a form that binds with high affinity, and that few dyneins attach to *oda16* axonemes because of a dynein defect, outer arm dynein was extracted from *oda16* axonemes, concentrated to approximate the dynein levels of a wild-type extract, and then tested for its ability to bind to *oda16* axonemes. Blots show that outer arm dyneins were restored to near wild-type abundance in this experiment, and electron microscopy confirmed that a normal outer row dynein density was restored (Fig. 2, D–F). Thus, there are no apparent problems with either the axonemal binding sites or the dynein that can bind to those sites in *oda16* flagella.

Dynein preassembly in oda16 cytoplasm

We next examined the role of ODA16 in cytoplasmic preassembly of outer arm dynein. Although data from dikaryon rescue experiments are consistent with the presence of intact, preassembled dynein in *oda16* cytoplasm (Ahmed and Mitchell, 2005), we considered an alternative hypothesis. The ODA16 protein that is supplied to *oda16* mutant cytoplasm during dikaryon formation might be rapidly converting dynein from a non-preassembled form into one that is preassembled and able to be transported into flagella. We previously demonstrated that soluble extracts of wild-type cells, made by glass bead disruption in the absence of detergent, contain outer row dynein proteins preassembled into a complex that includes all three heavy

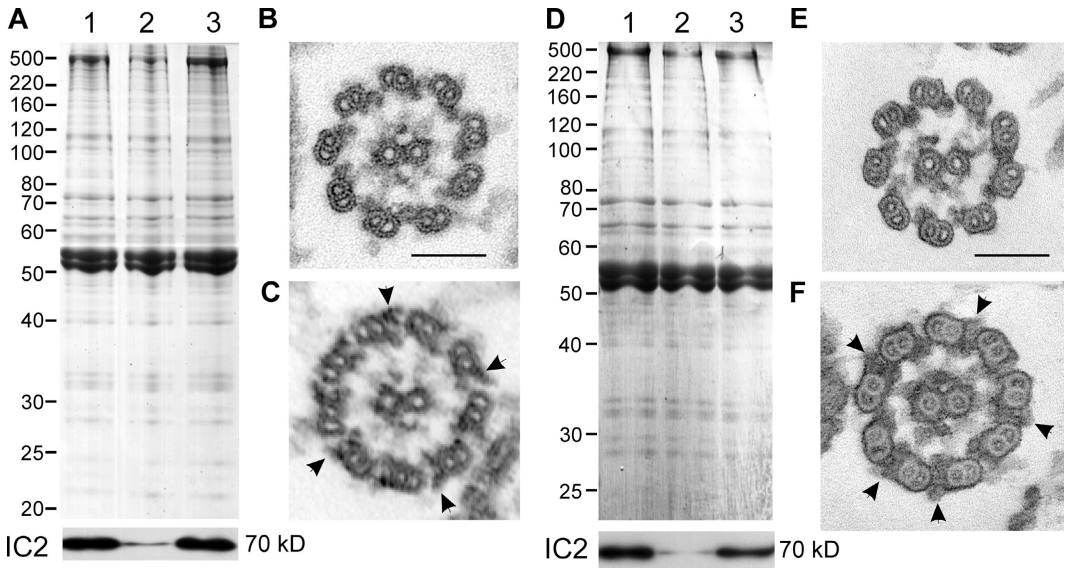

Figure 2. **Outer arm dynein binds onto *oda16* axonemes in vitro.** (A) A Coomassie blue–stained SDS-PAGE gel of wild-type axonemes (1), *oda16* axonemes (2), and *oda16* axonemes combined 1:1 with a dynein-containing extract from wild type axonemes (3), and a Western blot (bottom) of the same protein samples probed with an antibody against ODA-IC2, showing restoration of outer arm dynein on the *oda16* axonemes to wild-type levels. A comparison between electron micrographs of cross sections through an *oda16* axoneme (B) and an *oda16* axoneme incubated with a wild-type dynein extract (C) shows that a full complement of outer arm dyneins (C, arrows) were restored to the *oda16* axonemes incubated with the wild-type dynein extract. The same preparations were used for the gel samples in lanes 2 and 3 of A and for the electron microscopy samples in B and C. (D) A Coomassie blue–stained SDS-PAGE gel of wild-type axonemes (lane 1), *oda16* axonemes (lane 2), and *oda16* axonemes treated with a dynein-containing extract from *oda16* axonemes that had been concentrated threefold (lane 3), and a corresponding Western blot (bottom) was probed with an anti–ODA-IC2 antibody. Outer arm dynein has been restored on the *oda16* axonemes to near-wild-type levels. Electron microscopy cross sections of the material used for lane 2 (E) and lane 3 (F) show that a nearly wild-type complement of outer arm dyneins (F, arrows) were restored on the *oda16* axoneme after incubation with concentrated *oda16* dynein extract. Numbers adjacent to gel blot panels indicate the estimated mass in kD of each detected band. Bars, 100 nm.

chains and both intermediate chains (Fowkes and Mitchell, 1998). In extracts from some dynein assembly mutants, such as *oda7*, these subunits fail to preassemble, and some individual subunits show reduced cytoplasmic abundance, whereas in other mutants, such as docking complex mutant *oda1*, all subunits appear at normal abundance and in a stable complex. To assess dynein subunit stability in *oda16* cytoplasm, blots of cytoplasmic extracts were probed with antibodies to the five larger outer row dynein proteins. All five proteins show an increase in abundance in an *oda16* extract compared with their levels in extracts of wild-type or *oda4* (outer arm dynein heavy chain β [ODA-HCβ] mutant) cells (Fig. 3 A), and this increase in dynein subunit abundance is rescued back to wild-type levels by expression of an ODA16HA transgene. We previously showed that the HA-tagged *ODA16* transgene phenotypically complements the *oda16* assembly defect and that ODA16HA is expressed in *ODA16-1R(HA)* flagella at levels comparable to that of ODA16 in wild-type cells (Ahmed and Mitchell, 2005). These changes in heavy chain abundance can be observed directly in a Coomassie blue–stained gel (Fig. 3 A, top, HC) and by immunoblotting (Fig. 3 A, bottom). Probing this blot with anti-ODA16 shows that the ODA16 protein is expressed at wild-type levels in the *oda4* cytoplasm, that no ODA16 is seen in the cytoplasm of *oda16* cells, and that only the higher molecular weight HA-tagged ODA16 protein appears in the *ODA16-1R(HA)* strain. The increase in dynein abundance seen in *oda16* cytoplasmic extracts correlates well with the increase seen by immunofluorescence in *oda16* cell bodies (Fig. 1 B), and suggests that all of the dynein destined for flagellar assembly is synthesized in *oda16* cells but accumulates in the cytoplasm because of its inefficient transport into the flagellar compartment.

To determine the assembly state of dynein subunits in these cytoplasmic extracts, ODA-HCβ was immunoprecipitated with an anti-HCβ monoclonal antibody. Western blots show that a complex containing all of the major outer arm dynein subunits was coprecipitated by this antibody from both wild-type and *oda16* extracts (Fig. 3 B), which indicates that these subunits were successfully preassembled in the absence of the ODA16 protein. No subunits were precipitated from wild-type extracts by an unrelated anti-HA monoclonal antibody (Fig. 3 B, Ig lane) or from *oda4* extracts by the anti-HCβ antibody (Fig. 3 B, *oda4* lane). Immunoprecipitates of ODA16HA from *ODA16-1R(HA)* extracts failed to coprecipitate dynein proteins, and likewise, outer arm dynein immunoprecipitates from *ODA16-1R(HA)* cells contained no detectable ODA16HA protein (not depicted), which indicates that ODA16 is unlikely to be associated with dynein in this cytoplasmic pool.

To assess the ability of these preassembled dynein complexes to bind to axonemal docking sites, cytoplasmic extracts were mixed with axonemes from the outer row dynein assembly mutant *pf28*, an ODA-HCγ mutant. In these experiments, a cytoplasm/flagella stoichiometric ratio of 2:1 was used, based on previous work showing that the apparent size of the cytoplasmic pool of flagellar precursors is sufficient for assembly of half-length flagella in the presence of protein synthesis inhibitors (Rosenbaum et al., 1969). As shown by the reappearance of normal levels of dynein heavy chains by a Coomassie stain (Fig. 3 C, top) and of all tested subunits by Western blots (Fig. 3 C, bottom),

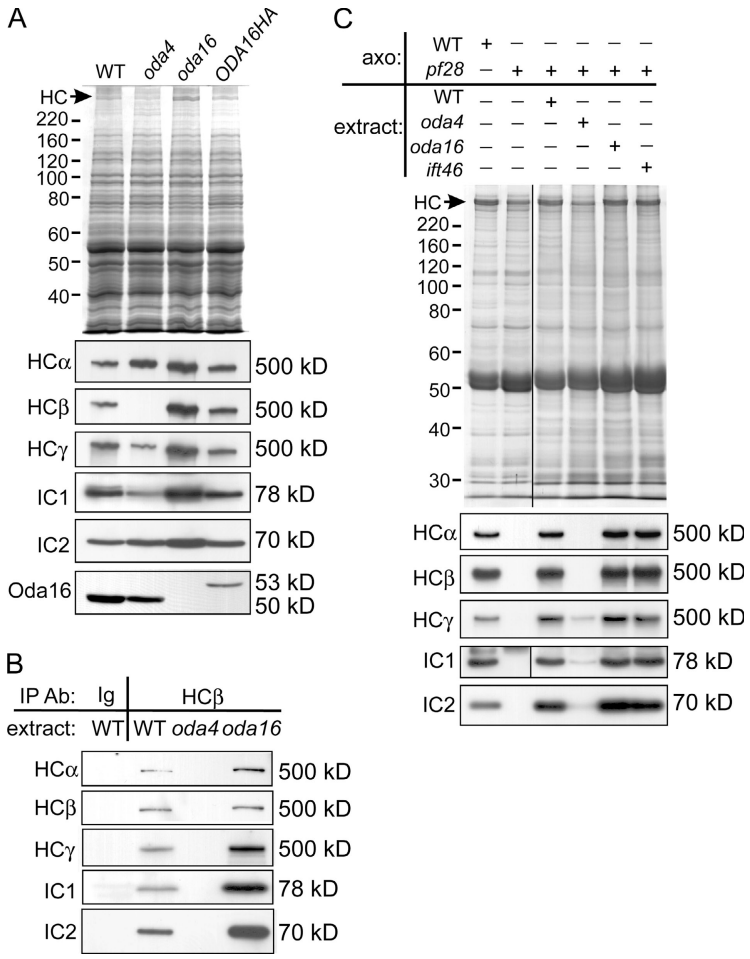

Figure 3. **ODA16 is not needed for dynein preassembly in the cytoplasm.** (A) Western blots demonstrate subunit abundance in wild-type and mutant cytoplasmic extracts. HCβ mutant *oda4* lacks HCβ but retains normal levels of other dynein subunits and ODA16 protein. The *oda16* extract lacks ODA16 and has abnormally high levels of dynein subunits. Expression of ODA16HA in the *oda16* cells (*ODA16HA)* restores dynein subunits to wild-type levels. Note the increased size of ODA16 due to the HA tag. (B) Axonemal outer row dynein subunits are preassembled in *oda16* cytoplasm. Immunoprecipitation of dynein with anti-HCβ coprecipitates all three heavy chains and both intermediate chains from both wild-type (WT) and *oda16* cytoplasmic extracts. Mock precipitation from the wild type with anti-HA (Ig) and from *oda4* with anti-HCβ failed to precipitate any subunits. (C) Axonemal dynein in *oda16* cytoplasm is competent to bind to axonemes. Stained gels and blots of axonemes from the wild type (WT) or *pf28* cells separated by SDS-PAGE show that *pf28* axonemes completely lack outer row dynein (first two lanes). To test the ability of axonemal dynein in the cytoplasmic pool to bind to axonemes, *pf28* axonemes and cytoplasmic extracts were incubated together at a 1:2 stoichiometric ratio for 1 h, and washed axonemes were analyzed (last four lanes). Outer arm dynein proteins in wild-type, *oda16*, and *ift46* extracts, but not *oda4* extracts, were competent to bind to *pf28* axonemes and restore dynein to wild-type levels. The stained gel and IC1 blot in C used identical sample loads; the first two lanes were originally run on the same gel as other lanes, but intervening lanes have been spliced out (indicated by black vertical lines). Gels used to prepare blots of all three HCs and IC2 in C were prepared with fivefold less protein than is shown in the gel. In addition to the mass of size standards, the position of dynein heavy chains (HC) is indicated by an arrow next to the stained gel images in A and C. Numbers adjacent to gel blot panels indicate the estimated mass in kD of each detected band.

the wild-type extract supported assembly of normal amounts of dynein onto *pf28* axonemes. In contrast, an *oda4* extract supported assembly of no HCα and only very small amounts of IC1, IC2, and HCγ, even though these subunits are present at approximately wild-type levels in the *oda4* cytoplasm (Fig. 3 A). Dynein from the *oda16* extract bound robustly to the *pf28* axonemes. The ability of this dynein to bind when cytoplasm and axonemes are mixed in vitro, bypassing the need for a transport step, indicates that the ODA16 protein is not needed to make an assembly competent preassembled dynein complex, but only to facilitate the transport of this complex into the flagellar compartment. Because the *ift46* mutant was also reported to be defective for outer dynein arm assembly (Hou et al., 2007), we included a cytoplasmic extract from this strain in our axoneme-binding experiment. As with *oda16*, the *ift46* extract contained dynein that was able to bind with *pf28* axonemes in vitro to restore all tested outer arm dynein subunits (see Fig. 3 C, last lane).

ODA16 localization

Biochemical fractionation of flagella has shown that ODA16 resides primarily in the flagellar matrix and does not copurify with axonemal outer arm dynein (Ahmed and Mitchell, 2005). To better understand the mechanism by which this protein affects outer arm dynein assembly, we visualized its distribution in cells by immunofluorescence and Western blotting. When wild-type *C. reinhardtii* were double labeled with anti-ODA16 and anti-acetylated tubulin antibodies, ODA16 was seen to localize predominantly to the peribasal body region, with weaker staining seen throughout the entire flagellar length (Fig. 4, A and B). This distribution is strikingly different from outer arm dynein distribution, which is mostly in the flagella starting above the transition zone and dispersed in the cytoplasm (Fig. 1), but is similar to that seen for several IFT components including the IFT kinesin subunit FLA10 (Vashishtha et al., 1996). To directly compare ODA16 and FLA10 localization, *oda16* cells expressing HA-tagged ODA16 were double labeled with anti-FLA10 and anti-HA antibodies. By immunofluorescence, the distribution of ODA16HA is unchanged by the addition of the tag, and ODA16HA and FLA10 approximately colocalize in both the flagella and the peribasal body region (Fig. 4 C).

To compare the relative abundance of ODA16 in flagella and cytoplasm, blots of whole cell protein were compared with protein from equal numbers of deflagellated cell bodies and with flagella isolated from an equal number of cells (Fig. 4 D). Blots of 10-fold and 50-fold higher amounts of flagella samples were included to provide a semiquantitative comparison. ODA16 appears to be at least 50-fold more abundant in the cytoplasm than in flagella, somewhat similar to the distribution of an IFT complex B protein (IFT46), which is between 10-fold and 50-fold more abundant in cytoplasm, whereas axonemal ODA-IC2 appears about equally abundant in cell body and flagellar fractions.

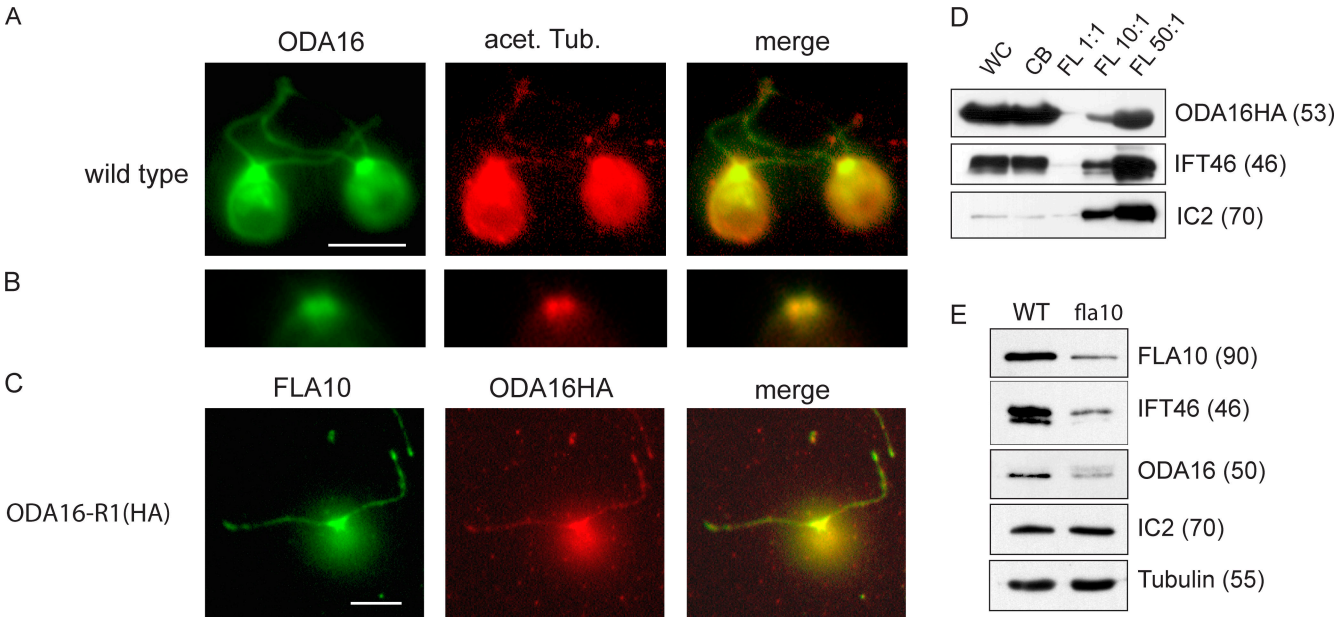

Figure 4. **ODA16 distribution is similar to the distribution of IFT proteins.** Wild-type *C. reinhardtii* (A and B) were probed with antibodies against ODA16 and acetylated tubulin. ODA16 appears in both the flagella and the cytoplasm, with a concentration around the basal bodies. A merged image of ODA16 and acetylated tubulin staining shows colocalization along the length of the flagella. (B) Localization at the peribasal body region is shown at higher magnification. (C) The *oda16-1R(HA)* strain, which expresses an HA-tagged version of ODA16, was probed with antibodies against IFT kinesin (FLA10) and HA (ODA16HA). A merged image of FLA10 and HA staining shows colocalization along the length of the flagella as well as brighter staining in the peribasal body region. (D) Western blots of cell fractions show that ODA16 is an abundant protein in cytoplasmic fractions. Protein samples prepared from whole cells (WC), deflagellated cell bodies (CB), and flagella (FL) of strain *ODA16-R1(HA)* were loaded at equal stoichiometry (1:1) or at a 10- or 50-fold excess of flagella. Both IFT46 and ODA16 are 20–50-fold more abundant in cytoplasm, whereas axonemal dynein (IC2) is nearly equally abundant in cytoplasm and flagella fractions. (E) A Western blot of wild type (WT) and *fla10*^{ts} flagella blotted with antibodies against an IFT kinesin subunit (FLA10), an IFT complex B protein (IFT46), and ODA16 shows that all three are reduced in the *fla10*^{ts} flagella. Outer row dynein (IC2) is unaffected by this partial reduction in ODA16. Tubulin was used as a loading control. Numbers adjacent to gel blot panels indicate the estimated mass in kD of each detected band. Bars, 5 μm.

In temperature-sensitive flagellar assembly strain *fla10*^{ts}, IFT subunit abundance in flagella is reduced even at the permissive temperature because of a reduction in FLA10 kinesin levels, but enough IFT is maintained to support assembly of full-length flagella whose axonemal structure and motility remain wild type (Pedersen et al., 2006). ODA16 levels in *fla10*^{ts} flagella were compared with levels in wild-type flagella to determine if ODA16 localization to the flagella is dependant on FLA10 kinesin activity. As illustrated in Fig. 4 E, ODA16 levels were reduced in *fla10*^{ts} flagella, as were levels of IFT46 and FLA10, whereas levels of axonemal ODA-IC2 remained normal. These results show that ODA16 levels in flagella depend on transport into the flagellar compartment by IFT, and suggest that ODA16 maintains its flagellar abundance through association with the FLA10 kinesin or another IFT complex protein.

We previously found that ODA16 enters flagella in the absence of outer arm dynein (Ahmed and Mitchell, 2005), thus ODA16 is likely to interact directly with the IFT machinery for its transport rather than indirectly through an association with dynein, and its abundance and distribution in the flagellar compartment should not be directly linked to that of assembled outer row dyneins. To test these assumptions, dikaryons were formed by mating *ODA16-1R(HA)* (tagged ODA16, wild type for outer row dynein assembly) with *oda2* (untagged ODA16, defective for outer row dynein assembly), and the distribution of outer row dynein and ODA16HA were visualized by immunofluorescence 40 min and 140 min after mixing cells (Fig. 5). Immediately after cell fusion (15 min after mixing cells), both outer row dynein (IC2) and ODA16 were present in flagella from the *ODA16-1R(HA)* cell, but neither protein was present in flagella from the *oda2* cell (unpublished data). After 40 min, ODA16HA was present around both pairs of basal bodies and within both pairs of flagella, whereas outer arm dynein was still only detectable in one pair of flagella (Fig. 5, A–C). By 140 min, ODA16HA and outer arm dynein were both detectable in all four flagella (Fig. 5, D–F). The outer arm dynein signal intensity in the *oda2* flagella increased gradually between ~40 and 90 min after mating, and was uniformly distributed along the flagellar length at all time points examined. In summary, we conclude that ODA16 is present in both cytoplasmic and flagellar compartments, that its abundance is much greater in the cytoplasm than in flagella, and that its distribution is independent of dynein distribution but similar to, and dependent on, IFT complex distribution.

Oda16 yeast two-hybrid screen

To identify proteins that interact with ODA16, we conducted a yeast two-hybrid screen, and used mammalian resources to take advantage of the high overall level of sequence similarity (>70%) between algal and mammalian ODA16 homologues. A human ODA16 cDNA was subcloned into a yeast two-hybrid vector and used as bait to screen a mouse testis–derived cDNA library. The 168 clones initially selected for growth dependence on a

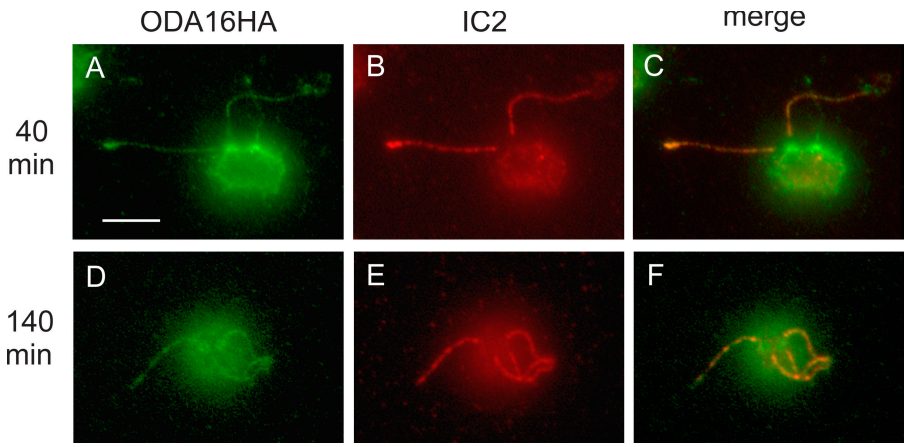

Figure 5. **ODA16 enters the flagella at a faster rate than outer arm dynein.** *Oda16-1-R(HA)* X *oda2* dikaryons were prepared 40 and 140 min after mating. Dikaryons were probed with rat anti-HA (green) to visualize ODA16HA (A and D) and mouse anti–ODA-IC2 (red) to visualize outer arm dynein (B and E). By 40 min, ODA16HA is detected in all visible flagella and both sets of basal bodies, whereas ODA-IC2 is only detectable in the two flagella from the *Oda16-1R(HA)* parent and as a diffuse cytoplasmic signal. By 140 min, ODA16HA and ODA-IC2 are detectable in all four flagella. Merged images (C and F) show colocalization of ODA16 and IC2 along flagella, but only ODA16 appears concentrated around basal bodies. Bar, 5 µm.

Gal4 promoter driven by the two-hybrid interaction were retested for expression of a Gal4-dependent β-galactosidase gene. DNA was recovered from 13 colonies positive for expression of both two-hybrid reporter genes, and sequencing revealed four independent clones, which encoded mouse homologues of a cytoplasmic protein (pellino2), a mitochondrial protein (creatine kinase), and two flagellar proteins (inner arm dynein light chain p28 and IFT complex B subunit IFT46). One representative of each clone was reintroduced into yeast and crossed with either a control strain carrying the empty Gal4 DNA-binding domain vector or a strain carrying a vector expressing the ODA16-Gal4 DNA-binding domain fusion protein. Only the IFT46 clone retained a positive signal on retesting (Fig. 6 B), whereas p28 showed a false positive signal when combined with the empty vector (Fig. 6 A). All three selected two-hybrid *Mm*IFT46 cDNA sequences contained full-length coding sequences in frame with the Gal4 activation domain, and also contained sequences from the 5′ untranslated region of *Mm*IFT46 that added linkers of up to 125 amino acids between the Gal4 activation domain and IFT46.

Although mouse and human ODA16 sequences are highly conserved, *Mm*IFT46 and *Cr*IFT46 share only 36% identity and 50% similarity (Fig. 6 C). To confirm that the *C. reinhardtii* homologues of ODA16 and IFT46 interact, pull-down assays were conducted with bacterially expressed proteins. ODA16 with an amino-terminal GST tag and IFT46 with an amino-terminal HIS tag were coexpressed, and $IFT46^{HIS}$ was purified from bacterial extracts with nickel-coated magnetic beads. Blots show that $IFT46^{HIS}$ could pull down $ODA16^{GST}$ but not GST alone (Fig. 6 D), which supports the the conclusion that these two proteins interact directly in vitro. In a reciprocal experiment, $IFT46^{HIS}$ copurified with $ODA16^{GST}$ but not with GST alone (unpublished data). As a further test of the ability of ODA16 to interact with native IFT46, $ODA16^{GST}$ was used to pull down interacting proteins from an NP-40-generated flagellar extract containing flagellar matrix proteins. As illustrated in Fig. 5 E, IFT46 was precipitated with $ODA16^{GST}$ but not with GST alone.

In vivo interaction between ODA16 and IFT particles

To confirm that these *Chlamydomonas* proteins interact in vivo, detergent-generated flagellar matrix extracts from the HA-tagged *ODA16-1R(HA)* strain were immunoprecipitated with anti-HA antibodies. Blots of the resulting pellets show that IFT complex B (IFT46 and IFT81) and the FLA10 IFT motor are specifically coprecipitated with ODA16HA (Fig. 6 F). In contrast, outer arm dynein subunits were not detectable in these precipitates (unpublished data). Collectively, these results support a model in which an association between ODA16 and the IFT complex, mediated at least in part by a direct interaction between ODA16 and IFT46, is essential for efficient transport of outer arm dynein into the flagellar compartment, but dynein itself, once it reaches the matrix, does not remain associated with this IFT–ODA16 complex.

Discussion

Outer arm dynein assembly is a multistep process that involves preassembly of subunits in the cytoplasm, movement of complexes into flagella, and assembly of these complexes into a functional dynein arm. Most mutations that disrupt this process have been traced to genes encoding subunits of the dynein motor itself or subunits of complexes that form binding sites for motor attachment, but *oda16* appears to be an exception. Based on this and our previous studies, ODA16 should not be considered a new dynein subunit or docking site protein, as it is not needed to form a functional motor complex or docking complex (Ahmed and Mitchell, 2005), does not partition biochemically as an axonemal protein, and has a distribution resembling that of IFT proteins, not axonemal proteins (Fig. 4). We demonstrate here that ODA16 is also unlikely to function as a chaperone at the outer doublet attachment step, as it is not needed to make an assembly competent binding site or to make an assembly competent dynein (Fig. 2). ODA16 is also not required to chaperone the preassembly of dynein subunits in the cytoplasm because complexes are preassembled in *oda16* cytoplasm and are competent to bind to axonemes (Fig. 3). Instead, ODA16 appears to be needed only for efficient transport of outer arm dynein motor complexes into the flagellar compartment. Because low levels of outer arm dynein manage to assemble in the absence of ODA16 (Ahmed and Mitchell, 2005), we conceive the role of ODA16 to be a cofactor or adaptor that enhances the ability of the IFT machinery to transport outer arm dynein.

Several other axonemal components, including the inner arm dyneins and radial spokes, have been shown to enter the

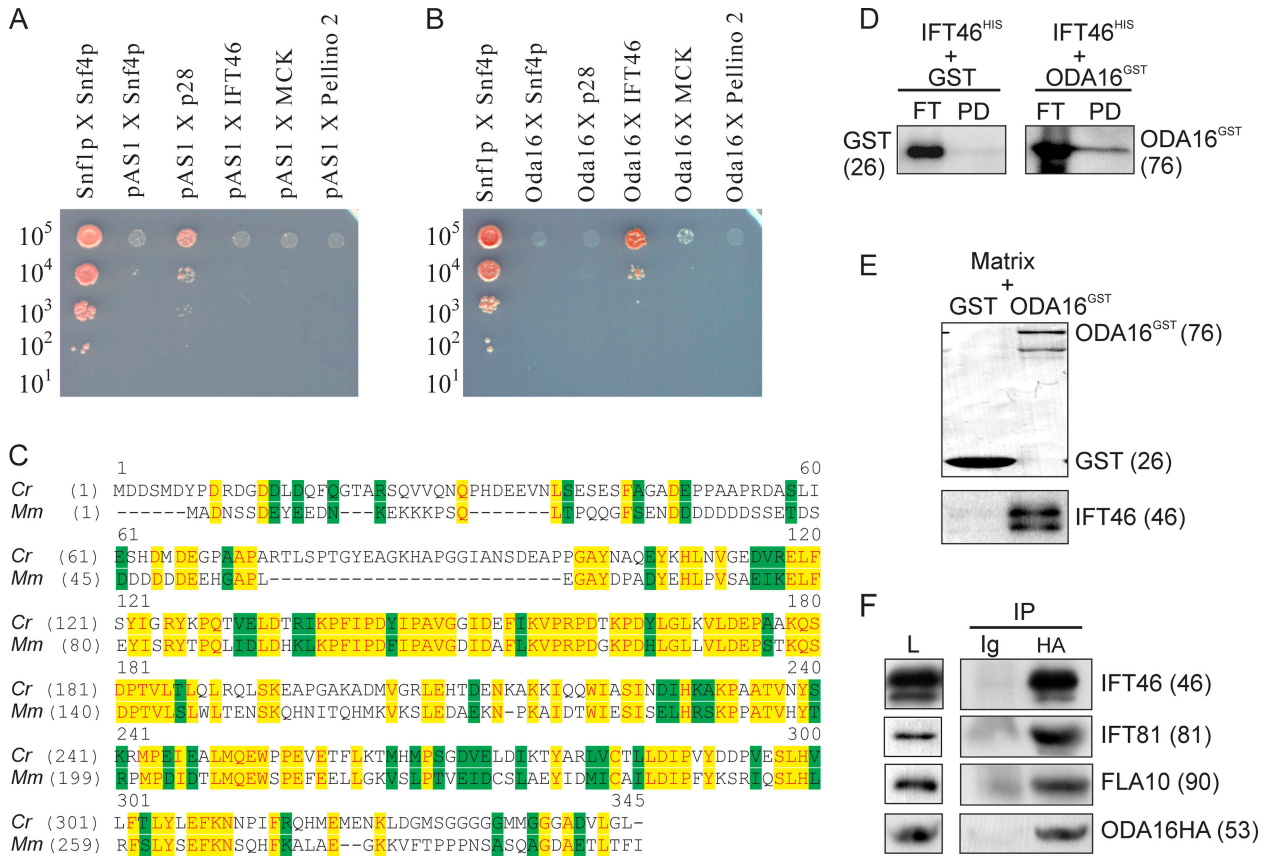

Figure 6. **ODA16 interacts with IFT46.** (A and B) A yeast two-hybrid screen shows that the mouse IFT46 homologue interacts with human ODA16. A dilution series from diploid *S. cerevisiae* containing one representative of each positive clone from a mouse testis cDNA Gal4AD library screen, as well as a control vector pAS1CYH2 (Gal4BD only; A) or a vector expressing *Hs*ODA16-Gal4BD (B), were grown on 25-mM 3,5-aminotriazole plates. The mouse p28 homologue showed a moderate interaction with the Gal4BD alone (A) and no interaction with *Hs*ODA16-Gal4BD (B), whereas mouse IFT46 showed a moderate interaction with *Hs*ODA16-Gal4BD (B) and none with Gal4BD alone (A). Two other clones selected in earlier screening steps, mitochondrial creatine kinase and pellino 2, both failed to show a significant interaction with ODA16-Gal4BD (B). Snf1p in pAS1CYH2 and Snf4p in pACTII were included as a positive control. The approximate number of cells spotted is indicated on the left. (C) *C. reinhardtii* IFT46 (*Cr*) shares 36% identity (yellow) and 50% similarity (green) with mouse IFT46 (*Mm*). The three positive yeast two-hybrid clones contain full-length *Mm*IFT46 cDNA. Accession nos. are DQ151642 for *Cr*IFT46 and BC080764 for *Mm*IFT46. (D) Pull-down experiments using bacterially expressed ODA16 and IFT46 show that these proteins interact in vitro. Either GST or ODA16^{GST} were coexpressed in *E. coli* with IFT46^{HIS}. Coexpressed GST and IFT46^{HIS}, or ODA16^{GST} and IFT46^{HIS} were pulled down using nickel-coated magnetic particles. Western blot analysis on flow-through (FT) and pull-down (PD) fractions probed with the anti-GST antibody shows that ODA16^{GST}, but not GST alone, copurified with IFT46^{HIS}. (E) Pull-down of native IFT46 from flagellar matrix. GST and GST-ODA16 fusion proteins were incubated with flagellar matrix prepared from wild-type strain 137c. A blot of proteins in each precipitate was stained for total protein (top) and probed with anti-IFT46 (bottom). Unlike GST alone, GST-ODA16 was able to pull down IFT46 from flagellar matrix. (F) Coprecipitation of ODA16 and IFT subunits from flagellar matrix. Matrix from *Oda16-1R(HA)* cells was immunoprecipitated with anti-HA monoclonal 12CA5 (lane HA) or with a nonspecific control Ig, and blots of the resulting precipitates were probed with antibodies to the indicated proteins (anti-HA 12CA5 for ODA16HA). Blots show coprecipitation of IFT complex B proteins (IFT46 and IFT81) and IFT kinesin (FLA10) with ODA16HA. Lane L shows the amount of each protein in 20% of the extract used for precipitations. Numbers adjacent to gel blot panels indicate the estimated mass in kD of each detected band.

flagellar compartment as partially assembled complexes and to require IFT for incorporation into flagella. In contrast, evidence of a role for IFT in outer dynein arm assembly has been questioned. Piperno et al. (1996), using cytoplasmic complementation in dikaryons between strains that carried the temperature-sensitive IFT kinesin mutation, *fla10^{ts}*, concluded that outer row dynein could assemble after IFT had been blocked by a temperature shift, whereas inner row dynein could not. In that study, mating was used to fuse a gamete carrying a dynein assembly defect with a gamete that was wild type for dynein assembly, and the recovery of dynein into the mutant flagella was analyzed by immunofluorescence. However, recent experiments with *fla10^{ts}* strains have shown that IFT is required for downstream signaling steps essential to mating-based cell fusion in *Chlamydomonas* (Wang et al., 2006), and therefore, the mated cells analyzed by Piperno et al. (1996) likely retained at least a small residual IFT activity that could have supported outer dynein arm assembly. Thus, assembly of inner and outer row dyneins may both require IFT yet differ in some essential aspect of the transport mechanism such as the need to reach the flagellar tip for cargo release.

Axonemal protein assembly is thought to depend on transport from a peribasal body loading zone to the flagellar tip (Qin et al., 2004; Pedersen et al., 2006), but outer arm dyneins could be an exception. Concentration at a peribasal body location has been described for inner row dynein light chain p28 (Piperno et al., 1996), intermediate chain IC138 (Hou et al., 2007), and radial spoke protein 3 (Qin et al., 2004), but outer row dynein displays no such concentrated peribasal body localization (Fig. 1;

see also Piperno et al., 1996; Hou et al., 2007). Assembly of tubulin onto a growing flagellum has been shown to occur at the tip (Rosenbaum and Child, 1967; Johnson and Rosenbaum, 1992), and when axonemal complexes such as inner row dyneins (Piperno et al., 1996) or radial spokes (Johnson and Rosenbaum, 1992) assemble onto existing flagella in vivo after gamete fusion, they also begin binding at the tip, and gradually assemble in a distal–proximal gradient. In similar cell fusion experiments, however, outer row dynein binds simultaneously along the entire flagellar length through a mechanism that apparently does not require IFT-assisted transport to the flagellar tip (Piperno et al., 1996). If radial spokes and inner row dyneins cannot pass between doublet microtubules, access to preexisting binding sites is likely limited to the flagellar tip. These cargos may retain an association with IFT particles until they reach the flagellar tip, where IFT particles are remodeled, before being released. In contrast, axonemal binding sites for outer row dynein are readily accessible along the outside of axonemes so that assembly can occur along the entire flagellum simultaneously. Thus, outer row dynein may only require IFT for movement from the cytoplasm into the flagellum, where it could be released immediately. We have been unable to detect an association between dynein and ODA16 by immunoprecipitation of either ODA16 or of outer arm dynein from flagellar matrix extracts. Another recent study (Rompolas et al., 2007) also found that outer row dynein does not coprecipitate with IFT proteins from flagellar matrix. It is therefore likely that ODA16 protein performs a transport role unique to proteins that do not require transport to the tip for their assembly, a category that may include matrix proteins and membrane proteins, as well as proteins associated with the outer surface of doublet microtubules such as outer row dynein.

Hou et al. (2007) showed that IFT46, a core IFT B protein, is necessary for outer row dynein assembly, and we provide evidence that ODA16 aids outer row dynein assembly through its association with IFT46 (Fig. 6). We also show that outer arm dynein subunits in the *ift46* strain, like those in an *oda16* strain, are retained in the cytoplasm in a form that is fully able to assemble onto *pf28* axonemes in vitro (Fig. 3 C), which supports a conclusion that *oda16* and *ift46* block dynein assembly at a similar stage. Should ODA16 be considered a peripheral IFT subunit? ODA16 has a cellular distribution similar to that of IFT complexes (Figs. 4 and 5), an abundance within the flagellar compartment that is dependent on IFT complexes (Fig. 4 D), and an ability to copurify with IFT particles in vivo (Fig. 6). However, mutations at the *oda16* locus, unlike those in core IFT proteins such as IFT88 (Pazour et al., 2002) and IFT46 (Hou et al., 2007), primarily affect outer row dynein assembly, and have no affect on flagellar length or on the flagellar abundance of IFT subunits. In addition, homologues of ODA16 are only seen in organisms with motile axonemes that retain outer row dynein (Ahmed and Mitchell, 2005). Thus, if ODA16 is an IFT subunit, it is not a subunit essential for any common role of IFT particles in the assembly and maintenance of flagella as organelles but instead functions as an IFT-associated adaptor for a specific peripheral axonemal component, the outer dynein arm. ODA16 sequence is highly conserved, and the interaction between ODA16 and IFT46 seen in *Chlamydomonas* flagellar extracts was initially detected through two-hybrid analysis of mammalian proteins (Fig. 5 A), thus, this interaction is likely to have evolved before the divergence of plants and animals from their last common ancestor.

Our results suggest that axonemal outer arm dynein must associate with IFT proteins, aided by ODA16, for transport into the flagellar compartment, but only during a brief transit through the flagellar transition zone. Thus far we have been unsuccessful in observing complexes containing both ODA16 and outer arm dynein proteins, or IFT and outer arm dynein proteins, in cytoplasmic extracts by immunoprecipitation. In the cytoplasm, ODA16 is concentrated in the peribasal body region (Fig. 4), whereas outer arm dynein appears to be evenly distributed throughout the cytoplasm (Fig. 1), which suggests that only a small portion of preassembled dynein associates with cytoplasmic ODA16 and IFT complexes at any one time. Because the transition zone remains with the cell body during induced deflagellation (Sanders and Salisbury, 1989), the flagellar matrix fraction that we and others have analyzed only contains IFT complexes that have moved beyond the transition zone and thus likely released their outer arm dynein cargo. It is unclear at this time if IFT particles from the transition zone are represented in our cytoplasmic extracts; however, this transition zone fraction would be difficult to detect against the background of total cytoplasmic IFT proteins, which outnumber IFT proteins in the 12-µm-long flagella by at least 20-fold (Fig. 4) and would be expected to outnumber those in the 0.5-µm-long transition zone by ∼500-fold.

Specific proteins or targeting sequences needed for recognition of axonemal cargoes by the IFT machinery have not been identified, and no direct interactions have been previously described between IFT subunits and axonemal cargoes. Although we have not as yet characterized its interaction with dynein, we hypothesize that ODA16 plays a role specific for proteins that do not require transport to the flagellar tip for their assembly, perhaps by assisting in the association of such cargoes with IFT particles around basal bodies and their subsequent release upon entry into the flagellar compartment. Similar to the adaptors for other intracellular transport processes, ODA16 could mediate changes in affinity with the transport machinery as the cargo moves from one compartment to another. Screens for assembly mutations that affect axonemal components such as outer arm dyneins have not been saturated, as only single alleles exist at several dynein assembly loci; for some of these loci, gene products have not been identified. It is therefore likely that other axonemal structures are transported into the flagellar compartment through interactions with IFT adaptors that are functionally similar to ODA16.

Materials and methods

C. reinhardtii strains

Strain *137c* served as genetic background and wild-type control for all experiments. Additional strains used include *oda2(pf28)* (Mitchell and Rosenbaum, 1985), *fla10*^{ts} (Walther et al., 1994), *oda16-1* and *oda16-1R(HA)* (Ahmed and Mitchell, 2005), *oda4* (Okagaki and Kamiya, 1986), and *ift46* (Hou et al., 2007).

Protein extraction and fractionation

Flagella and flagellar fractions were prepared as described previously (Ahmed and Mitchell, 2005). High-salt extracts prepared from *137c* or *oda16* axonemes were dialyzed against HMDEK (30 mM Hepes, 5 mM

$MgSO_4$, 1 mM DTT, 0.5 mM EGTA, and 25 mM potassium acetate, pH 7.4) for 18 h at 4°C. For outer arm dynein rebinding experiments, the dialyzed extract was incubated with *oda16* axonemes in HMDEK for 2 h on ice and sedimented in a microcentrifuge for 15 min.

To compare relative protein abundance in whole cells, cell bodies, and flagella, protein was prepared from equal numbers of cells before or immediately after pH shock deflagellation (Witman, 1986) by resuspending pelleted cells in a small volume of water and precipitating proteins with 3 volumes of acetone. Flagella were prepared from a known number of cells by dibucaine deflagellation (Witman, 1986) and appropriately diluted to provide SDS-PAGE samples of known stoichiometry relative to whole cell and cell body samples.

Cytoplasmic extracts were made from autolysin-dewalled cells by washing cells in HMDEK50 (HMDEK prepared with 50 mM potassium acetate), suspending $\sim 2 \times 10^9$ cells with 1.5 ml of HMDEK50, and vortexing with 1.5 ml of 0.5-mm glass beads in a 15-ml conical tube (three times for 1 min). Broken cells were spun in a microcentrifuge (Hermle) for 30 min, and supernates were frozen in liquid N_2 and stored at −70°C for later use. For binding of cytoplasmic proteins to *pf28* axonemes, extract from 6 × 10^8 cells was diluted to 0.5 ml with HMDEK50, mixed with axonemes prepared from 3 × 10^8 cells, and incubated on ice for 1 h. Axonemes were pelleted, washed with 1 ml HMDEK50, and prepared for SDS-PAGE.

Antibodies and immunodetection

Antibodies used include anti-acetylated tubulin (clone 6-11B-1; Sigma-Aldrich), affinity-purified rabbit anti-ODA16 (Ahmed and Mitchell, 2005), mouse monoclonal anti–ODA-HCβ (C11.6), anti–ODA-IC1 (C1.1), anti–ODA-IC2 (C11.4; Mitchell and Rosenbaum, 1986), mouse monoclonal anti–ODA-HCγ (12γB; a gift of S.M. King, University of Connecticut Health Center, Farmington, CT; King et al., 1985), rabbit polyclonal anti–ODA-HCα (B3B; Fowkes and Mitchell, 1998), mouse monoclonal anti-HA epitope 12CA5 (Roche), rat monoclonal anti-HA epitope 3F10 (Roche), rabbit anti-GST (Sigma-Aldrich), rabbit anti-FLA10 (a gift of J.L. Rosenbaum, Yale University, New Haven, CT; Kozminski et al., 1995), rabbit anti-IFT81 and -IFT139 (Cole et al., 1998), and rabbit anti-IFT46 (a gift of H. Qin, Texas A&M University, College Station, TX; Hou et al., 2007). For blots, proteins separated by SDS-PAGE were transferred onto a polyvinylidene fluoride membrane (Immobilon-P; Millipore), and peroxidase-labeled secondary antibodies were detected on Biomax Light film (Kodak) using Super Signal West Dura Extend Duration Substrate (Thermo Fisher Scientific). Molecular mass was estimated based on migration of Benchmark protein ladder (Invitrogen) standards. Scanned images of stained gels and films were generated in Photoshop 6.0 (Adobe). Indirect immunofluorescence followed previously described methods (Cole et al., 1998). Alexa Fluor 488 goat anti–rabbit and Alexa Fluor 555 goat anti–mouse secondary florescent antibodies were used at a 1:1,000 dilution (Invitrogen). Images were visualized using a microscope (microphot-FX; Nikon) using a 60× 1.40 NA plan Apo objective (Nikon), and captured using Spot Advance 4.0.0 software (Diagnostic Instruments, Inc.). Images were cropped and adjusted using Photoshop 6.0.

Electron microscopy

Specimens for thin section electron microscopy were prepared as previously described (Mitchell and Sale, 1999). Images were taken using a microscope (100CXII; JEOL Ltd.) operated at 80 kV. Negatives were scanned and imported in Photoshop 6.0, inverted, and adjusted for contrast and median density.

Yeast two-hybrid screen

The coding region of a full-length cDNA clone of the human ODA16 homologue (available from GenBank/EMBL/DDBJ under accession no. BC036377; clone ID 4824989; Thermo Fisher Scientific) was amplified using the primers GenNde1f (5′-GCAAGCATATGAAGCTCAAGAGC-3′), which adds an NdeI site before the start codon, and GenBam1r (5′-CTAGCAAGGATCCTCACTGACC-3′), which adds a BamHI site after the stop codon. The PCR product was cloned between NdeI and BamHI in the yeast Gal4-binding domain vector pAS1-CYH2 to create pAC1-CYH2-HsODA16. An amplified sample of a mouse testis-derived cDNA library cloned into Gal4 activation domain vector pACTII was provided by S. Dutcher (Washington University in St. Louis, St. Louis, MO). Vector plasmid pAS1-CYH2, control plasmids pSE111 (pACTII containing SNF4) and pSE112 (pAS1-CYH2 containing SNF1), and *Saccharomyces cerevisiae* strains Y190 (mating type a) and Y187 (mating type α) were provided by D. Amberg (State University of New York Upstate Medical University, Syracuse, NY). All pAS1-CYH2–based constructs were transformed into strain Y190, and pACTII-based constructs (including the library) were transformed into strain Y187.

Before conducting the screen, the following tests were performed to confirm that pAC1-CYH2-HsODA16 did not autoactivate. Y187/Y190 diploids between pAS1-CYH2 and pACTII-based plasmids were replica plated onto plates containing 10 mM, 25 mM, 50 mM, or 100 mM 3,5-aminotriazole (Irving et al., 1995), and scored for growth. A high level of growth confirmed the pSE111 and pSE112 interaction, whereas pSE111 failed to show any interaction with pAS1-CYH2-HsODA16 on plates containing 25 mM, 50 mM, or 100 mM 3,5-aminotriazole. HsODA16-Gal4BD localization to the nucleus was also confirmed by immunofluorescence.

The yeast two-hybrid screen was conducted as described previously (Clark et al., 2006) with the following alterations. 3.5 × 10^8 Y190 cells containing pAS1-CYH2-HsODA16 were transformed with the mouse cDNA library (3.5 × 10^6 clones) and plated onto SD + 25 mM 3,5-aminotriazole + 10 μg/ml adenine. Of 101 survivors, 18 rescored as positive for a lacZ gene driven by a Gal4-dependent promoter. DNA was recovered from 13 lacZ-positive clones strains and sequenced, and we identified four independent clones encoding an uncharacterized protein (available from GenBank/EMBL/DDBJ under accession no. BC010326) with homology to *Cr*IFT46 (three clones), an axonemal dynein light chain (accession no. BC118619) with homology to *Cr*p28 (one clone), pellino 2 (accession no. NM_033602), which lacks algal homologues (one clone), and mitochondrial creatine kinase 2 (accession no. NM_198415; eight clones). Y190 cells containing pAS1-CYH2 or pAS1-CYH2-HsODA16 were mated with Y187 cells containing one representative of each positive clone from the screen. As a positive control, pSE112- and pSE111-containing strains (SNF4–SNF1 interaction) were included. After growth in Sc-Leu-Trp medium for 6 d, a dilution series was spotted onto selection plates (25 mM 3,5-aminotriazole + 10 μg/ml adenine) and scored after 6 d.

Pull-down assays and immunoprecipitation

For pull-downs with bacterially expressed proteins, either pGEX-ODA16 (GST-tagged ODA16; Ahmed and Mitchell, 2005) or pGEX-4T-2 (GST alone) were cotransformed into BL21LysDE3 *Escherichia coli* with pRSF-Duet1-IFT46F (HIS-tagged IFT46). The full coding sequence of *Chlamydomonas* IFT46 was subcloned into pRSF-Duet using the EcoRI and SalI sites of MCS-1. HIS tag–based pull-down assays were performed using the MagneHis Protein Purification System (Promega) according to the manufacture's instructions, except that 500 mM NaCl was added to all buffers used for the Ni-based pull-downs. Protein was separated and transferred as described for immunodetection. For pull-downs and immunoprecipitations of proteins expressed in *Chlamydomonas*, flagellar matrix was prepared by freeze-thaw as described previously (Ahmed and Mitchell, 2005). GST and GST-ODA16p fusion proteins were incubated with wild-type flagellar matrix, and precipitated proteins were blotted using polyclonal anti-IFT46. For anti-HA immunoprecipitation, 400 μg of flagellar matrix from *oda16-1R(HA)* was precleared with protein A/G agarose (Santa Cruz Biotechnology, Inc.) followed by incubation with either normal mouse IgG (Santa Cruz Biotechnology, Inc.) or monoclonal anti-HA antibody 12CA5 (Roche) for 2 h, and precipitation with 20 μl of protein A/G agarose for 1 h on ice. Blots of immunoprecipitates were probed with polyclonal anti-IFT46, monoclonal anti-IFT81, polyclonal anti-FLA10, or monoclonal anti-HA antibodies. For immunoprecipitation of cytoplasmic proteins, precleared cytoplasmic extracts from $\sim 10^9$ cells were incubated with 2 μg of mouse monoclonal anti-HA (as a control Ig) or mouse monoclonal anti-HCβ C11.6 (to precipitate proteins coassembled with HCβ).

We thank Judy Freshour and Brandy Verhalen for their help in making constructs; Masako Nakatsugawa for electron microscopy; Susan Dutcher for the yeast two-hybrid library; David Amberg, Michael Clark, and Brandy Verhalen for their help with the yeast two-hybrid screen; George Witman for the *ift46* strain; and Hongmin Qin and Joel Rosenbaum for the FLA10 and IFT46 antibodies.

We acknowledge National Institutes of Health grants to D.R. Mitchell (GM44228) and D.G. Cole (GM61920).

Submitted: 4 February 2008
Accepted: 10 September 2008

References

Ahmed, N.T., and D.R. Mitchell. 2005. ODA16p, a *Chlamydomonas* flagellar protein needed for dynein assembly. *Mol. Biol. Cell.* 16:5004–5012.

Clark, M.G., J. Teply, B.K. Haarer, S.C. Viggiano, D. Sept, and D.C. Amberg. 2006. A genetic dissection of Aip1p's interactions leads to a model for Aip1p-cofilin cooperative activities. *Mol. Biol. Cell.* 17:1971–1984.

Cole, D.G. 2003. The intraflagellar transport machinery of *Chlamydomonas reinhardtii*. *Traffic.* 4:435–442.

Cole, D.G., D.R. Diener, A.L. Himelblau, P.L. Beech, J.C. Fuster, and J.L. Rosenbaum. 1998. *Chlamydomonas* kinesin-II-dependent intraflagellar transport (IFT): IFT particles contain proteins required for ciliary assembly in *Caenorhabditis elegans* sensory neurons. *J. Cell Biol.* 141:993–1008.

Dutcher, S.K. 2003. Elucidation of basal body and centriole functions in *Chlamydomonas reinhardtii*. *Traffic.* 4:443–451.

Fowkes, M.E., and D.R. Mitchell. 1998. The role of preassembled cytoplasmic complexes in assembly of flagellar dynein subunits. *Mol. Biol. Cell.* 9:2337–2347.

Hou, Y., H. Qin, J.A. Follit, G.J. Pazour, J.L. Rosenbaum, and G.B. Witman. 2007. Functional analysis of an individual IFT protein: IFT46 is required for transport of outer dynein arms into flagella. *J. Cell Biol.* 176:653–665.

Irving, M., T. St Claire Allen, C. Sabido-David, J.S. Craik, B. Brandmeier, J. Kendrick-Jones, J.E.T. Corrie, D.R. Trentham, and Y.E. Goldman. 1995. Tilting of the light-chain region of myosin during step length changes and active force generation in skeletal muscle. *Nature.* 375:688–691.

Johnson, K.A., and J.L. Rosenbaum. 1992. Polarity of flagellar assembly in *Chlamydomonas*. *J. Cell Biol.* 119:1605–1611.

Kamiya, R. 2002. Functional diversity of axonemal dyneins as studied in *Chlamydomonas* mutants. *Int. Rev. Cytol.* 219:115–155.

King, S.M., T. Otter, and G.B. Witman. 1985. Characterization of monoclonal antibodies against *Chlamydomonas* flagellar dyneins by high-resolution protein blotting. *Proc. Natl. Acad. Sci. USA.* 82:4717–4721.

Kozminski, K.G., P.L. Beech, and J.L. Rosenbaum. 1995. The *Chlamydomonas* kinesin-like protein FLA10 is involved in motility associated with the flagellar membrane. *J. Cell Biol.* 131:1517–1527.

Li, J.B., J.M. Gerdes, C.J. Haycraft, Y. Fan, T.M. Teslovich, H. May-Simera, H. Li, O.E. Blacque, L. Li, C.C. Leitch, et al. 2004. Comparative genomics identifies a flagellar and basal body proteome that includes the BBS5 human disease gene. *Cell.* 117:541–552.

Mitchell, D.R., and J.L. Rosenbaum. 1985. A motile *Chlamydomonas* flagellar mutant that lacks outer dynein arms. *J. Cell Biol.* 100:1228–1234.

Mitchell, D.R., and J.L. Rosenbaum. 1986. Protein-protein interactions in the 18S ATPase of *Chlamydomonas* outer dynein arms. *Cell Motil. Cytoskeleton.* 6:510–520.

Mitchell, D.R., and W.S. Sale. 1999. Characterization of a *Chlamydomonas* insertional mutant that disrupts flagellar central pair microtubule-associated structures. *J. Cell Biol.* 144:293–304.

Okagaki, T., and R. Kamiya. 1986. Microtubule sliding in mutant *Chlamydomonas* axonemes devoid of outer or inner dynein arms. *J. Cell Biol.* 103:1895–1902.

Pazour, G.J., S.A. Baker, J.A. Deane, D.G. Cole, B.L. Dickert, J.L. Rosenbaum, G.B. Witman, and J.C. Besharse. 2002. The intraflagellar transport protein, IFT88, is essential for vertebrate photoreceptor assembly and maintenance. *J. Cell Biol.* 157:103–113.

Pazour, G.J., N. Agrin, J. Leszyk, and G.B. Witman. 2005. Proteomic analysis of a eukaryotic cilium. *J. Cell Biol.* 170:103–113.

Pedersen, L.B., S. Geimer, and J.L. Rosenbaum. 2006. Dissecting the molecular mechanisms of intraflagellar transport in *Chlamydomonas*. *Curr. Biol.* 16:450–459.

Piperno, G., K. Mead, and S. Henderson. 1996. Inner dynein arms but not outer dynein arms require the activity of kinesin homologue protein $KHp1^{FLA10}$ to reach the distal part of flagella in *Chlamydomonas*. *J. Cell Biol.* 133:371–379.

Qin, H., D.R. Diener, S. Geimer, D.G. Cole, and J.L. Rosenbaum. 2004. Intraflagellar transport (IFT) cargo: IFT transports flagellar precursors to the tip and turnover products to the cell body. *J. Cell Biol.* 164:255–266.

Rompolas, P., L.B. Pedersen, R.S. Patel-King, and S.M. King. 2007. *Chlamydomonas* FAP133 is a dynein intermediate chain associated with the retrograde intraflagellar transport motor. *J. Cell Sci.* 120:3653–3665.

Rosenbaum, J.L., and F.M. Child. 1967. Flagellar regeneration in protozoan flagellates. *J. Cell Biol.* 34:345–364.

Rosenbaum, J.L., J.E. Moulder, and D.L. Ringo. 1969. Flagellar elongation and shortening in *Chlamydomonas*. The use of cycloheximide and colchicine to study the synthesis and assembly of flagellar proteins. *J. Cell Biol.* 41:600–619.

Sanders, M.A., and J.L. Salisbury. 1989. Centrin-mediated microtubule severing during flagellar excision in *Chlamydomonas reinhardtii*. *J. Cell Biol.* 108:1751–1760.

Scholey, J.M. 2003. Intraflagellar transport. *Annu. Rev. Cell Dev. Biol.* 19:423–443.

Silflow, C.D., and P.A. Lefebvre. 2001. Assembly and motility of eukaryotic cilia and flagella. Lessons from *Chlamydomonas reinhardtii*. *Plant Physiol.* 127:1500–1507.

Vashishtha, M., Z. Walther, and J.L. Hall. 1996. The kinesin-homologous protein encoded by the *Chlamydomonas FLA10* gene is associated with basal bodies and centrioles. *J. Cell Sci.* 109:541–549.

Walther, Z., M. Vashishtha, and J.L. Hall. 1994. The *Chlamydomonas FLA10* gene encodes a novel kinesin-homologous protein. *J. Cell Biol.* 126:175–188.

Wang, Q., J. Pan, and W.J. Snell. 2006. Intraflagellar transport particles participate directly in cilium-generated signaling in *Chlamydomonas*. *Cell.* 125:549–562.

Wirschell, M., G. Pazour, A. Yoda, M. Hirono, R. Kamiya, and G.B. Witman. 2004. Oda5p, a novel axonemal protein required for assembly of the outer dynein arm and an associated adenylate kinase. *Mol. Biol. Cell.* 15:2729–2741.

Witman, G.B. 1986. Isolation of *Chlamydomonas* flagella and flagellar axonemes. *Methods Enzymol.* 134:280–290.

Zariwala, M.A., M.R. Knowles, and H. Omran. 2007. Genetic defects in ciliary structure and function. *Annu. Rev. Physiol.* 69:423–450.